

# Effective capacity analysis of configurable intelligent surface-assisted NOMA communications systems

Huu Q. Tran<sup>1</sup>, Ho Van Khuong<sup>2,3</sup>

<sup>1</sup>Faculty of Electronics Technology, Industrial University of Ho Chi Minh (IUH), Ho Chi Minh City, Vietnam

<sup>2</sup>Department of Telecommunications Engineering, Ho Chi Minh City University of Technology (HCMUT), Ho Chi Minh City, Vietnam

<sup>3</sup>Vietnam National University Ho Chi Minh City, Vietnam

## Article Info

### Article history:

Received Aug 30, 2023

Revised Nov 16, 2023

Accepted Dec 7, 2023

### Keywords:

Base station

Configurable intelligent surface

Effective capacity

Non-orthogonal multiple access

Quality of service

Simultaneous transmitting and reflecting

## ABSTRACT

This paper investigates the integration of configurable intelligent surfaces (CIS) into relay radio networks, focusing on communication system enhancement. Towards this end, we propose CIS-assisted non-orthogonal multiple access (NOMA) communication systems to improve direct connections between a base station and two destination nodes. Our primary objective is to assess the network's overall capacity, considering critical factors like signal-to-noise ratio, the number and placement of CIS components, quality of service exponent, and power distribution coefficients. Analytical equations developed in this research closely align with simulation results, validating our theoretical analysis. This study underscores the growing significance of CISs in modern communication systems, introducing adaptability and optimization to wireless networks. By exploring CIS-assisted NOMA communication systems, we contribute to discussions about the evolving landscape of wireless communication technologies, poised to revolutionize information transmission and reception in the digital age.

This is an open access article under the [CC BY-SA](https://creativecommons.org/licenses/by-sa/4.0/) license.



## Corresponding Author:

Huu Q. Tran

Faculty of Electronics Technology, Industrial University of Ho Chi Minh

12 Nguyen Van Bao Street, Ward 4, Go Vap District, Ho Chi Minh, Vietnam

Email: tranquyhuu@iuh.edu.vn

## 1. INTRODUCTION

Non-orthogonal multiple access (NOMA) is employed in wireless communications systems for multiple access to drastically improve spectral efficiency and efficiently allocate radio resources. In conventional orthogonal multiple access (OMA) paradigms like frequency division multiple access and time division multiple access, each device is allocated exclusive frequency bands or time slots. However, multiple devices share same time-frequency resources concurrently in NOMA, enabling more efficient utilization of the available spectrum. In NOMA, two major techniques are applied: superposition coding (SC) and successive interference cancellation (SIC). SC is an information theory and digital communication technique that enables the simultaneous transmission of multiple messages over a single channel. It optimizes channel capacity by encoding signals in a manner that allows for receivers to separate and decode NOMA signals. This approach is valuable in various scenarios, including multi-user communication, broadcast channels, and cognitive radio systems, where efficient use of the channel's capacity is crucial. SIC is conducted to detach and detect signals at the receiver in NOMA communications systems. Moreover, NOMA can provide more fairness among users by

serving both near and far devices simultaneously, ensuring that all users get some level of service. Therefore, NOMA has been emerged as a promising solution for modern wireless communications systems, particularly in the context of fifth-generation (5G) and beyond. It can enhance efficiency and capacity of wireless networks and accommodate the increasing demand for data-intensive applications and services [1]–[9].

Meanwhile, configurable intelligent surface (CIS), also known as reconfigurable intelligent surface (RIS) or intelligent reflecting surface (IRS), has received attention as a potential technology in wireless communications that can be used to manipulate and control radio waves [10], [11]. It includes a planar array of passive components (such as antennas or metamaterial units) that can be electronically adjusted to modify the propagation of electromagnetic waves in real-time. Therefore, CIS has potential applications in various wireless communications scenarios, including internet of things (IoT) devices, 5G, and beyond, indoor wireless communications systems, and satellite communications [12], [13].

The combination of NOMA and CIS introduces new dimensions to wireless communications design, opening up avenues for even greater improvements in system capacity, coverage, and energy efficiency [14]–[16]. Li *et al.* [17] explores a downlink system featuring a RIS. This study's primary objective is to facilitate communication between a source and two users using NOMA techniques with RIS support. The research emphasizes the system's ability to support real-time services in future networks. It introduces a mathematical framework to analyze how different system parameters, including the quantity of IRS components and the presence of strong line-of-sight components, impact the performance of the IRS-aided system. The investigation of self-interference coefficients was conducted in [18]. Basar *et al.* [19] presents a comprehensive historical overview of cutting-edge solutions, aiming to clarify differences from other technologies. It highlights critical research challenges and the need to reevaluate communication-theoretic models in wireless networks when using RISs. The paper also analyzes theoretical performance limits using mathematical techniques and discusses potential applications in the context of sixth-generation (6G) and future wireless communications systems.

Our main objective is to evaluate system performance, focusing on the critical metric-effective capacity (EC)-for systems sensitive to latency constraints. Liu *et al.* [20] assessed NOMA networks using simultaneous transmission and reflection via simultaneous transmitting and reflecting (STAR)-RIS. They aimed to gauge the suitability of these networks for ultra-reliable low-latency communication. They also used EC as a key metric to evaluate latency requirements for NOMA users. Moreover, they derived analytical expressions for EC when a pair of NOMA users were positioned on opposite sides of the STAR-RIS. Additionally, their research incorporated high signal-to-noise ratio (SNR) slope and power offset for asymptotic analysis of ECs, particularly in scenarios with elevated SNR levels. The statistical quality of service (QoS) provided by IRS-assisted communication between a base station (BS) and user equipment (UE) was studied [21]. Aman *et al.* [21] the study in considered two different contexts: a multi-input single-output context, where the BS utilizes several antennas, and a single-input single-output context, where the BS is equipped with a single antenna.

In this paper, we delve into the intricate interplay between NOMA, CIS, and EC. EC is a valuable metric that characterizes achievable data rate under a certain QoS constraints, taking into account statistical properties of wireless channels and considering impacts of various impairments. The exploration of EC in the context of CIS-assisted NOMA communications systems provides valuable insights into potential gains and challenges of deploying these technologies in practical scenarios. By conducting such a comprehensive analysis, the paper sheds light on the tradeoffs between achievable rates and transmission parameters, thereby aiding in optimization and design of next-generation wireless systems. The subsequent sections of this paper delve into theoretical foundations, system model, mathematical formulation, and numerical results, ultimately contributing to the advancement of our understanding of capabilities of CIS-assisted NOMA communications systems. Accordingly, this paper contributes to the ongoing discourse on enhancing wireless communications systems by harnessing the synergy between NOMA and CIS technologies. The subsequent sections present a thorough examination of key concepts and methodologies, supported by rigorous analysis and simulation results. Through the lens of EC, this paper offers a deeper comprehension of potential benefits and challenges of deploying CIS-assisted NOMA communications systems, which has not been found in the open literature, eventually paving the way for informed decision-making in design and implementation of future wireless networks. The key contributions of this research are summarized as :

- Derivation of closed-form formulas for the EC of CIS-aided NOMA communications systems.
- Evaluation of impacts of parameters, namely the number of CIS elements ( $N$ ), QoS exponent ( $\nu$ ), average SNR ( $\rho$ ), and power allocation coefficient ( $a_1$ ) on the EC through numerical and simulation results. This evaluation provides insights into how changes in these parameters affect system performance. Moreover,

these influences serve as a foundation for selecting proper parameter values within the proposed system model to attain a trade-off among user satisfaction and performance metrics.

The rest of the paper keeps going with section 2 presenting the considered network model and channel statistics. Afterwards, section 3 analyzes effective capacity. Subsequently, section 4 discusses numerical and simulation results. Finally, section 5 gives conclusions.

*Notations:* capital bold letters are utilized to represent matrices, while lower bold letters represent vectors.  $\mathcal{CN}(\cdot, \cdot)$  represents a circularly symmetric complex gaussian distribution.  $|\cdot|$  represents the absolute value.  $\mathcal{P}[\cdot]$ , and  $\mathbb{E}[\cdot]$  denote the probability operator and the expectation operator, respectively. The superscripts  $(\cdot)^*$  and  $(\cdot)^H$  mean the conjugate and the hermitian transpose, correspondingly.  $I_K$  represents an identity matrix of size  $K \times K$ . Lastly, a diagonal matrix with components  $z_1, \dots, z_N$  along the diagonal is denoted as  $\text{diag}(z_1, \dots, z_N)$ .

## 2. CHANNEL STATISTICS AND SYSTEM MODEL

### 2.1. System description

This research involves the analysis of a CIS-enabled NOMA communications system in Figure 1. Where a BS employs a CIS to offer services to two users, each equipped with a single antenna, denoted as  $U_v$  where  $v \in \{1, 2\}$ . In such a system, CIS is a  $N$ -element reflecting metasurface and direct channels from BS to two devices ( $U_1$  and  $U_2$ ) are assumed to be available.

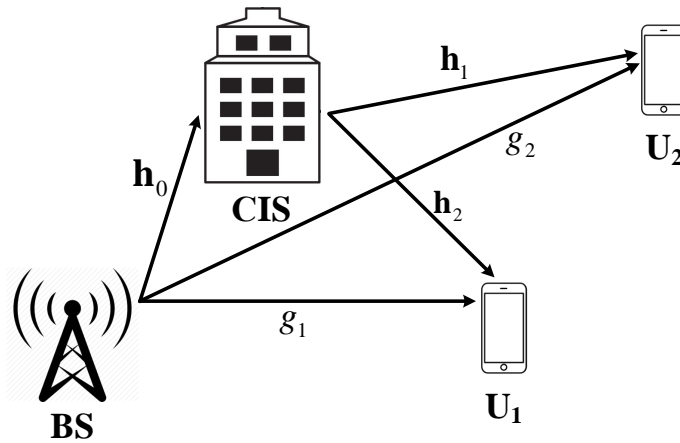


Figure 1. CIS-assisted NOMA communications systems

As shown in Figure 1, channel gains are denoted as follows: channel gain between BS and  $U_1$  is  $g_1$ , channel gain between BS and  $U_2$  is  $g_2$ , channel gain between BS and CIS is  $h_0$ , channel gain between CIS and  $U_1$  is  $h_1$ , and channel gain between CIS and  $U_2$  is  $h_2$ . Flat block fading channels are employed wherein they are quasi-static within each coherent interval. Moreover, we suppose they follow uncorrelated rayleigh fading with  $\lambda_{g_1}$ ,  $\lambda_{g_2}$ ,  $\lambda_{h_0}$ ,  $\lambda_{h_1}$  and  $\lambda_{h_2}$  representing large-scale fading coefficients of corresponding channels. Therefore, we infer  $g_1 \sim \mathcal{CN}(0, \lambda_{g_1})$ ,  $g_2 \sim \mathcal{CN}(0, \lambda_{g_2})$ ,  $h_0 \sim \mathcal{CN}(0, \lambda_{h_0} I_N)$ ,  $h_1 \sim \mathcal{CN}(0, \lambda_{h_1} I_N)$ , and  $h_2 \sim \mathcal{CN}(0, \lambda_{h_2} I_N)$ . Moreover, the phase-shift matrix for the link between CIS and BS is represented to be  $\Theta = \text{diag}(e^{j\chi_1}, e^{j\chi_2}, \dots, e^{j\chi_N})$ , wherein  $\chi_m \in [-\pi, \pi]$ ,  $\forall m$ , represents the phase-shift induced by the  $m^{\text{th}}$  element of CIS. During downlink transmission, BS transmits the following signal to  $U_1$  and  $U_2$ :

$$s = \sqrt{P_S a_1} s_1 + \sqrt{P_S a_2} s_2, \quad (1)$$

wherein  $P_S$  represents the transmission power of BS,  $a_1$  and  $a_2$  denote the fractions of  $P_S$  allocated to  $s_1$  and  $s_2$ , respectively, which are subject to the constraint  $a_1 + a_2 = 1$  and  $a_2 > a_1$ . It is important to note that  $s_1 \sim \mathcal{CN}(0, 1)$  and  $s_2 \sim \mathcal{CN}(0, 1)$  are messages intended for  $U_1$  and  $U_2$ , correspondingly. Here, our research focuses on two users in sub-6G networks to maintain generality. Therefore, the signal received by  $U_v$  from BS

through CIS is given by:

$$\begin{aligned} y_v &= (h_0^H \Theta h_v + g_v) s + n_v \\ &= (h_0^H \Theta h_v + g_v) \left( \sqrt{P_S a_1 s_1} + \sqrt{P_S a_2 s_2} \right) + n_v, \quad v \in \{1, 2\} \end{aligned} \quad (2)$$

where  $n_v \sim \mathcal{CN}(0, \sigma^2)$  represents the noise at the receive antenna. The signal-to-interference-plus-noise ratio (SINR) for decoding  $s_2$  at  $U_1$  is given by:

$$\begin{aligned} \gamma_{U_1}^{s_2} &= \frac{P_S a_2 |h_0^H \Theta h_1 + g_1|^2}{P_S a_1 |h_0^H \Theta h_1 + g_1|^2 + \sigma^2} \\ &= \frac{\rho a_2 |h_0^H \Theta h_1 + g_1|^2}{\rho a_1 |h_0^H \Theta h_1 + g_1|^2 + 1}, \end{aligned} \quad (3)$$

where  $\rho = \frac{P_S}{\sigma^2}$  denotes the average SNR at BS. For optimal phase-shifts, wherein  $\chi_m = \arg(g_v) - \arg([h_0^*]_m) - \arg([h_v^*]_m)$ ,  $\forall m$ , the instantaneous SINR in (3) can be formulated as (4):

$$\gamma_{U_1}^{s_2} = \frac{\rho a_2 \left| \sum_{n=1}^N |[h_0]_n| |[h_1]_n| + g_1 \right|^2}{\rho a_1 \left| \sum_{n=1}^N |[h_0]_n| |[h_1]_n| + g_1 \right|^2 + 1}. \quad (4)$$

For simpler manipulation, (4) can be rewritten as (5):

$$\gamma_{U_1}^{s_2} = \frac{\rho a_2 A_1}{\rho a_1 A_1 + 1}, \quad (5)$$

wherein  $A_v \triangleq \left| \sum_{n=1}^N |[h_0]_n| |[h_v]_n| + g_v \right|^2$ ,  $v \in \{1, 2\}$ , with  $[h_0]_n$  and  $[h_v]_n$  representing the  $n^{th}$  elements of  $h_0$  and  $h_v$ , respectively.

Subsequently, through the utilization of the SIC, we can formulate the SINR at  $U_1$ , which is used to decode its own signal  $s_1$ , as (6):

$$\gamma_{U_1}^{s_1} = \rho a_1 A_1. \quad (6)$$

Additionally, the SINR at  $U_2$ , used for decoding  $s_2$ , is calculated as (7):

$$\gamma_{U_2}^{s_2} = \frac{\rho a_2 A_2}{\rho a_1 A_2 + 1}. \quad (7)$$

Now, we can express achievable rates in bits/s/Hz for  $U_1$  and  $U_2$ , respectively, in CIS-assisted NOMA communications systems with direct links as (8):

$$\mathcal{R}_{U_1} = \log_2 (1 + \gamma_{U_1}^{s_1}) = \log_2 (1 + \rho a_1 A_1), \quad (8)$$

and

$$\mathcal{R}_{U_2} = \log_2 (1 + \gamma_{U_2}^{s_2}) = \log_2 \left( 1 + \frac{\rho a_2 A_2}{\rho a_1 A_2 + 1} \right). \quad (9)$$

## 2.2. Channel statistics

By utilizing the findings reported [22], one obtains the cumulative distribution function (cdf) of  $A_v$  to be:

$$F_{A_v}(x) = 1 - \frac{\Gamma(k_v, \sqrt{x}/w_v)}{\Gamma(k_v)} \quad (10)$$

wherein  $\Gamma(\cdot, \cdot)$  is the upper incomplete Gamma function and  $\Gamma(\cdot)$  represents the Gamma function [23]. The scale and shape parameters, respectively, for the cdf in (10):

$$w_v = \frac{4\lambda_{g_v} + 4N\xi\zeta_v^2 - \pi\lambda_{g_v}}{2(\sqrt{\pi\lambda_{g_v}} + 2N\xi\zeta_v)}, \quad (11a)$$

$$k_v = \frac{(\sqrt{\pi\lambda_{g_v}} + 2N\xi\zeta_v)^2}{4\lambda_{g_v} + 4N\xi\zeta_v^2 - \pi\lambda_{g_v}}, \quad (11b)$$

wherein  $\zeta_v = (4 - \pi^2/4) \sqrt{\lambda_{h_0}\lambda_{h_v}}/\pi$  and  $\xi = \pi^2/(16 - \pi^2)$ .

With the aid of [23] (8.354.2), we can derive (10) as (12):

$$F_{A_v}(x) = \frac{1}{\Gamma(k_v)} \sum_{q=0}^{\infty} \frac{(-1)^q x^{\frac{k_v+q}{2}}}{q! (k_v+q) w_v^{k_v+q}}. \quad (12)$$

Based on (12), one also expresses the probability density function of  $A_v$  to be:

$$f_{A_v} = \frac{\partial}{\partial x} F_{A_v}(x) = \frac{1}{2\Gamma(k_v)} \sum_{q=0}^{\infty} \frac{(-1)^q x^{\frac{k_v+q-2}{2}}}{q! w_v^{k_v+q}}. \quad (13)$$

### 3. EFFECTIVE CAPACITY ANALYSIS

The highest constant service rate that the service process may achieve while satisfying the target QoS is described as the effective capacity. It serves as an useful indicator for assessing the performance of delay-limited communications systems [24]. According to this definition, the effective capacity in bits/s/Hz of  $U_v$ ,  $v \in \{1, 2\}$ , is represented as (14):

$$\mathcal{E}_c^v = -\frac{1}{\nu_v TB} \ln(\mathbb{E}[e^{-\nu_v TB \mathcal{R}_{U_v}}]), \quad (14)$$

wherein  $T$  and  $B$  represent the block length and the bandwidth, respectively. The parameter  $\nu_v > 0$  is the QoS exponent, defined as (15):

$$\nu_v = -\lim_{z \rightarrow \infty} \frac{\ln(\mathcal{P}[L > z])}{z}, \quad (15)$$

wherein  $L$  denotes the equilibrium queue-length of the buffer at the transmitter. By plugging (8) and (9) into (14), one derives the effective capacity formulas for  $U_1$  and  $U_2$  as (16):

$$\mathcal{E}_c^1 = -\frac{1}{B_1} \log_2 \mathbb{E}[(1 + \rho a_1 A_1)^{-B_1}], \quad (16)$$

and

$$\mathcal{E}_c^2 = -\frac{1}{B_2} \log_2 \mathbb{E}\left[\left(1 + \frac{\rho a_2 A_2}{\rho a_1 A_2 + 1}\right)^{-B_2}\right], \quad (17)$$

where  $B_1 = (\nu_1 TB)/\ln 2$  and  $B_2 = (\nu_2 TB)/\ln 2$ .

The following Lemma presents the theoretical formulas for the effective capacities of  $U_1$  and  $U_2$ . These formulas are derived from the expressions in (16) and (17), while also considering the statistics of rayleigh fading channels. Lemma: the theoretical formulas of the effective capacities for  $U_1$  and  $U_2$  are provided, correspondingly, as (18) and (19):

$$\mathcal{E}_c^1 = -\frac{1}{B_1} \log_2 \left[ \frac{1}{2\Gamma(k_1)} \sum_{q=0}^{\infty} \frac{(-1)^q \Gamma\left(\frac{k_1+q}{2}\right) \Gamma\left(\frac{2B_1-k_1-q}{2}\right)}{q! w_1^{k_1+q} \Gamma(B_1) (\rho a_1)^{k_1+q-1}} \right], \quad (18)$$

$$\mathcal{E}_c^2 \approx -\frac{1}{B_2} \log_2 \left[ \frac{a_2 \pi}{4Pa_1 \Gamma(k_2)} \sum_{q=0}^{\infty} \sum_{p=1}^P \frac{(-1)^q \sqrt{1-v_p^2} \left( \frac{\Psi(t)}{\rho(a_2-a_1\Psi(t))} \right)^{\frac{k_1+q-2}{2}}}{q! w_2^{k_2+q} \left( 1 + \frac{\rho a_2 \Psi(t)}{\rho a_1 \Psi(t)+1} \right)^{B_1}} \right], \quad (19)$$

where  $\Psi(t) = \frac{a_2(t+1)}{2a_1}$  and  $v_p = \cos\left(\frac{2p-1}{2P}\pi\right)$ .

*Proof:* Firstly, we let  $\Lambda_1 = \rho a_1 A_1$  and substitute it into (16). Then, the expression of the effective capacity for  $U_1$  can be given explicitly as (20):

$$\mathcal{E}_c^1 = -\frac{1}{B_1} \log_2 \left[ \frac{1}{2\Gamma(k_1)} \sum_{q=0}^{\infty} \frac{(-1)^q}{q! w_1^{k_1+q} (\rho a_1)^{\frac{k_1+q-2}{2}}} \int_0^{\infty} (1 + \rho a_1 x)^{-B_1} x^{\frac{k_1+q-2}{2}} dx \right]. \quad (20)$$

After conducting several mathematical manipulations, the substitution of (13) into (20) leads to the final derivation of (18). Moreover, the representation of the effective capacity for  $U_2$  is expressed explicitly to be:

$$\begin{aligned} \mathcal{E}_c^2 &= -\frac{1}{B_2} \log_2 \left[ \int_0^{\infty} (1 + \Lambda_2)^{-B_2} f(\Lambda_2) d(\Lambda_2) \right] \\ &= -\frac{1}{B_2} \log_2 \left[ \frac{1}{2\Gamma(k_2)} \sum_{q=0}^{\infty} \frac{(-1)^q}{q! w_2^{k_2+q}} \int_0^{\frac{a_2}{a_1}} \left( 1 + \frac{\rho a_2 x}{\rho a_1 x + 1} \right)^{-B_1} \left( \frac{x}{\rho(a_2 - a_1 x)} \right)^{\frac{k_1+q-2}{2}} dx \right], \end{aligned} \quad (21)$$

where  $\Lambda_2 = \frac{\rho a_2 A_2}{\rho a_1 A_2 + 1}$ .

Now, we let  $t = \frac{2a_1}{a_2}x - 1$ . Then,  $\frac{a_2(t+1)}{2a_1} = x$  and hence,  $\frac{a_2}{2a_1}dt = dx$ . Accordingly, the effective capacity of  $U_2$  is expressed as (22):

$$\mathcal{E}_c^2 = -\frac{1}{B_2} \log_2 \left[ \frac{a_2}{4a_1\Gamma(k_2)} \sum_{q=0}^{\infty} \frac{(-1)^q}{q! w_2^{k_2+q}} \int_{-1}^1 \left( 1 + \frac{\rho a_2 \Psi(t)}{\rho a_1 \Psi(t) + 1} \right)^{-B_1} \left( \frac{\Psi(t)}{\rho(a_2 - a_1 \Psi(t))} \right)^{\frac{k_1+q-2}{2}} dt \right]. \quad (22)$$

Unfortunately, deriving an explicit formula for (22) is challenging. However, one can attain a precise approximation. Indeed, by utilizing Gaussian-Chebyshev quadrature [25] (25.4.38), we can achieve this as in (3.) with  $P$  representing complexity-accuracy tradeoff, thus completing the proof.

#### 4. RESULT AND DISCUSSION

To confirm the accuracy of the proposed derivations in section 3, we numerically simulate the effective capacity of CIS-assisted NOMA communications systems under practical circumstances. All simulation results are attained by taking the average of  $10^6$  simulation trials over rayleigh fading links. Unless otherwise addressed, simulation settings are configured to be  $N = 2$ ,  $a_1 = 0.1$ ,  $a_2 = 0.9$ ,  $B = 2$ ,  $T = 6.5$ ,  $\theta = 0.5$  and  $\lambda_{g_1} = \lambda_{g_2} = \lambda_{h_0} = \lambda_{h_1} = \lambda_{h_2} = 1$ .

For the quantity of CIS elements  $N = \{2, 4\}$ , we investigate the changes in effective capacities relative to the average SNR  $\rho$  in Figure 2. The results expose that the analytical findings and Monte-Carlo simulations are in an agreement, confirming the accuracy of the analysis in section 3. Moreover, in the range of low average SNRs, the effective capacity of  $U_2$  is considerably higher than that of  $U_1$ . Nonetheless, the performance tendency is reversed in the range of high average SNRs. Further, we observe that as the average SNR increases, the effective capacities of both  $U_1$  and  $U_2$  also increase. However, after the average SNR reaches a certain value, the effective capacity of  $U_2$  is saturated.

We present Figure 3 with the number of CIS elements considered as a variable to further investigate the relationship between the number of CIS elements and effective capabilities. It is observed that when the quantity of CIS elements accretes, the effective capacities of both  $U_1$  and  $U_2$  also increase. This outcome aligns with expectations, as the addition of more CIS elements leads to greater spatial diversity and improved user performance. Another noteworthy finding is that an increase in  $\rho$  results in enhanced user capacities. Particularly, it is demonstrated that when the quantity of CIS components is low, the value of  $\rho$  significantly impacts the effective capacity of  $U_2$ . However, once the quantity of CIS components reaches a certain threshold, the effective capacity of  $U_2$  ceases to rise in correlation with the number of CIS elements. This phenomenon occurs when  $N$  becomes large.

Figure 4 is presented to investigate the influence of the QoS exponent  $\nu_1 = \nu_2 = \nu$  upon effective capacities of  $U_1$  and  $U_2$ , considering  $\rho$  values of 10 dB and 15 dB. We have chosen the appropriate region

of  $\nu$  ranging from 0.2 to 2. As noted previously, a larger  $\nu$  indicates stricter delay limit, resulting in lower effective capacity. Consequently, one observes that when  $\nu$  increases, the effective capacities of both  $U_1$  and  $U_2$  decrease. Furthermore, it is evident that for low  $\nu$  values, both  $U_1$  and  $U_2$  experience a distinct reduction in effective capacities. This reduction is more pronounced for  $U_1$ . Additionally, we observe that the change in effective capacities becomes more gradual as  $\nu$  approaches 2. Further, the influence of higher  $\rho$  values on effective capacities excellently agrees with the findings in Figure 2.

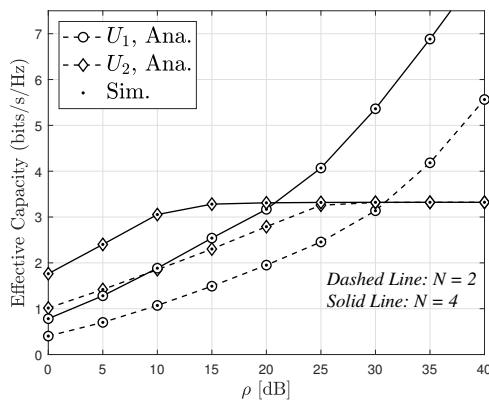


Figure 2. Effective capacities versus the average SNR  $\rho$

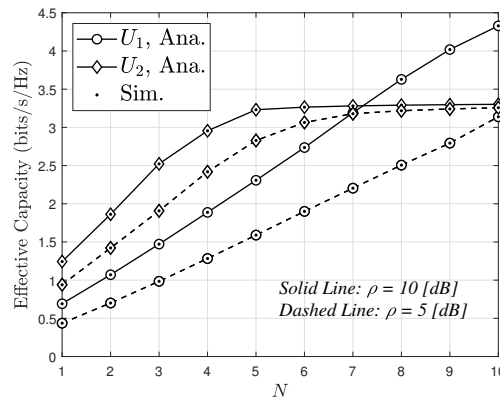


Figure 3. Effective capacities versus the quantity of CIS elements

Impacts of power allocation coefficients upon effective capacities of  $U_1$  and  $U_2$  are examined in Figure 5. We consider  $\rho$  values of 10 dB and 15 dB. As shown in Figure 5, increasing the power allocation coefficient for  $U_1$  results in a rise in  $U_1$ 's effective capacity, while decreases  $U_2$ 's effective capacity. This demonstrates that allocating more power to  $U_1$  leads to a higher level of the effective capacity for  $U_1$ . Notably, increasing  $\rho$  significantly enhances effective capacities, aligning with the findings in Figure 2. Furthermore, despite  $U_1$ 's lower initial effective capacity compared to that of  $U_2$ , the effective capacity of  $U_1$  surpasses that of  $U_2$  after the power allocation coefficient for  $U_1$  reaches a specific value. Based on the results in Figure 5, the optimum power allocation coefficient for the near device ( $a_1$ ) to maximize the network's total effective capacity is approximately 0.1.

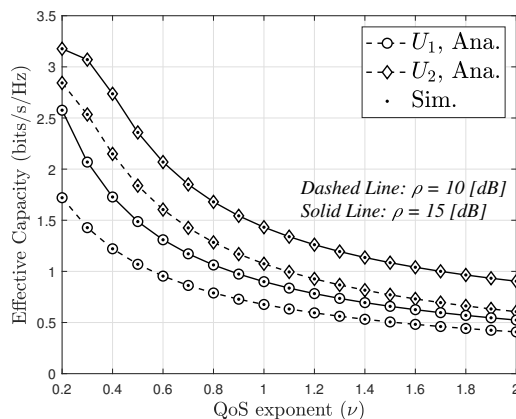


Figure 4. EC against the QoS exponent  $\nu$  and distinct  $\rho$  with ( $a_1 = 0.1$ ,  $a_2 = 0.9$ ) and the quantity of CIS elements ( $N = 2$ )

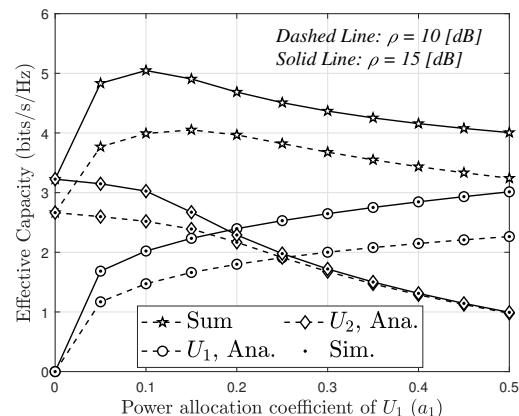


Figure 5. EC against the power allocation coefficient ( $a_1$ ) with the quantity of CIS elements ( $N = 3$ )

## 5. CONCLUSION

The performance of CIS-assisted NOMA communications systems was explicitly examined in this article using the metric of the effective capacity. We specifically developed closed-form formulas for the effective capacities of both users ( $U_1$  and  $U_2$ ) in these systems across rayleigh fading channels. The analytical closed-form equations and Monte Carlo simulations showed good agreement. Moreover, increasing the quantity of CIS elements enhances spatial diversity, leading to improved effective capacity. These analytical results provide valuable theoretical insights for CIS-assisted NOMA communications systems. In future studies, we will explore the impact of incorporating additional CIS processors into these systems to further ameliorate system performance.

## ACKNOWLEDGEMENT

Huu Q. Tran acknowledges the support of time and facilities from Industrial University of Ho Chi Minh City (IUH) for this study.

Ho Van Khuong acknowledges the support of time and facilities from Ho Chi Minh City University of Technology (HCMUT), VNU-HCM for this study.

## REFERENCES




- [1] H. Q. Tran, P. Q. Truong, C. V. Phan, and Q. T. Vien, "On the energy efficiency of NOMA for wireless backhaul in multi-tier heterogeneous CRAN," *2017 International Conference on Recent Advances in Signal Processing, Telecommunications Computing (SigTelCom)*, 2017, pp. 229-234, doi: 10.1109/SIGTELCOM.2017.7849827.
- [2] Z. Ding, X. Lei, G. K. Karagiannis, R. Schober, J. Yuan, and V. K. Bhargava, "A Survey on Non-Orthogonal Multiple Access for 5G Networks: Research Challenges and Future Trends," *IEEE Journal on Selected Areas in Communications*, vol. 35, no. 10, pp. 2181-2195, 2017, doi: 10.1109/JSAC.2017.2725519.
- [3] D. Wan, M. Wen, F. Ji, H. Yu, and F. Chen, "Non-orthogonal multiple access for cooperative communications: Challenges, opportunities, and trends," *IEEE Wireless Communications*, vol. 25, no. 2, pp. 109-117, 2018, doi: 10.1109/MWC.2018.1700134.
- [4] M. Liaqat, K. A. Noordin, T. A. Latef, and K. Dimyati, "Power-domain non orthogonal multiple access (PD-NOMA) in cooperative networks: an overview," *Wireless Networks*, vol. 26, pp. 181-203, 2020, doi: 10.1007/s11276-018-1807-z.
- [5] H. Q. Tran, T. T. Nguyen, C. V. Phan, and Q. T. Vien, "Power-splitting relaying protocol for wireless energy harvesting and information processing in NOMA systems," *IET Communications*, vol. 13, no. 14, pp. 2132-2140, 2019, doi: 10.1049/iet-com.2018.5897.
- [6] H. Q. Tran, C. V. Phan, and Q. T. Vien, "Power splitting versus time switching based cooperative relaying protocols for SWIPT in NOMA systems," *Physical Communication*, vol. 41, pp. 1-15, 2020, doi: 10.1016/j.phycom.2020.101098.
- [7] J. Li, H. H. Chen, and Q. Guo, "On the Performance of NOMA Systems With Different User Grouping Strategies," *IEEE Wireless Communications*, 2022, doi: 10.1109/MWC.010.2200185.
- [8] T. Le-Thanh and K. Ho-Van, "Non-orthogonal multiple access multiple input multiple output communications with harvested energy: Performance evaluation," *ETRI Journal*, 2023, pp. 1-14, doi: 10.4218/etrij.2023-0048.
- [9] N. S. Mouni, A. Kumar, and P. K. Upadhyay, "Adaptive User Pairing for NOMA Systems With Imperfect SIC," *IEEE Wireless Communications Letters*, vol. 10, no. 7, pp. 1547-1551, 2021, doi: 10.1109/LWC.2021.3074036.
- [10] H. Kim et al., "RIS-Enabled and Access-Point-Free Simultaneous Radio Localization and Mapping," *IEEE Transactions on Wireless Communications*, doi: 10.1109/TWC.2023.3307455.
- [11] Y. Zhu, Y. Liu, Q. Wu, C. You, and Q. Shi, "Channel Estimation By Transmitting Pilots From Reconfigurable Intelligent Surface," *IEEE Transactions on Wireless Communications*, doi: 10.1109/TWC.2023.3307450.
- [12] S. Ahmed and A. E. Kamal, "Sky's the Limit: Navigating 6G with A STAR-RIS for UAVs Optimal Path Planning," in *2023 IEEE Symposium on Computers and Communications*, pp. 582-587, 2023, doi: 10.1109/ISCC58397.2023.10218058.
- [13] S. Nassirpour, A. Vahid, D. T. Do, and D. Bharadia, "Beamforming Design in Reconfigurable Intelligent Surface-Assisted IoT Networks Based on Discrete Phase Shifters and Imperfect CSI," *IEEE Internet of Things Journal*, vol. 11, no. 3, pp. 5301-5315, 2024, doi: 10.1109/IJOT.2023.3305914.
- [14] Y. Liu, X. Mu, X. Liu, M. Di Renzo, Z. Ding, and R. Schober, "Reconfigurable Intelligent Surface-Aided Multi-User Networks: Interplay Between NOMA and RIS," *IEEE Wireless Communications*, vol. 29, no. 2, pp. 169-176, 2022, doi: 10.1109/MWC.102.2100363.
- [15] A. Chauhan, S. Ghosh, and A. Jaiswal, "RIS Partition-Assisted Non-Orthogonal Multiple Access (NOMA) and Quadrature-NOMA With Imperfect SIC," *IEEE Transactions on Wireless Communications*, vol. 22, no. 7, pp. 4371-4386, 2023, doi: 10.1109/TWC.2022.3224645.
- [16] T. Toregozhin, M. H. N. Shaikh, and G. Nauryzbayev, "Performance Analysis and Enhancement through Cooperative NOMA in STAR-RIS-aided Systems," *International Balkan Conference on Communications and Networking*, 2023, pp. 1-6, doi: 10.1109/BalkanCom58402.2023.10167959.
- [17] G. Li, H. Liu, G. Huang, X. Li, B. Raj, and F. Kara, "Effective capacity analysis of reconfigurable intelligent surfaces aided NOMA network," *EURASIP Journal on Wireless Communications and Networking*, vol. 2021, pp. 1-16, 2021, doi: 10.1186/s13638-021-02070-7.
- [18] S. Li, S. Yan, L. Bariah, S. Muhaidat, and A. Wang, "IRS-Assisted Full Duplex Systems Over Rician and Nakagami Fading Channels," *IEEE Open Journal of Vehicular Technology*, vol. 4, pp. 217-229, 2023, doi: 10.1109/OJVT.2022.3233857.
- [19] E. Basar, M. Di Renzo, J. De Rosny, M. Debbah, M. S. Alouini, and R. Zhang, "Wireless Communications Through Reconfigurable Intelligent Surfaces," *IEEE Access*, vol. 7, pp. 116753-116773, 2019, doi: 10.1109/ACCESS.2019.2935192.






- [20] H. Liu, G. Li, X. Li, Y. Liu, G. Huang, and Z. Ding, "Effective Capacity Analysis of STAR-RIS-Assisted NOMA Networks," *IEEE Wireless Communications Letters*, vol. 11, no. 9, pp. 1930-1934, 2022, doi: 10.1109/LWC.2022.3188443.
- [21] W. Aman, M. U. R. Mahboob, S. A. A. A. Nasir, K. Qaraqe, M. I. Ali, Q. H. Abbasi, "On the effective capacity of IRS-assisted wireless communication," *Physical Communication*, vol. 47, p. 101339, 2021, doi: 10.1016/j.phycom.2021.101339.
- [22] T. V. Chien et. al, "Coverage Probability and Ergodic Capacity of Intelligent Reflecting Surface-enhanced Communication Systems," *IEEE Communications Letters*, vol. 25, no. 1, pp. 69-73, 2021, doi: 10.1109/LCOMM.2020.3023759.
- [23] I. S. Gradshteyn and I. M. Ryzhik, *Table of Integrals, Series and Products*, 6th ed. New York, NY, USA: Academic Press, 2000.
- [24] D. Wu and R. Negi, "Effective capacity: a wireless link model for support of quality of service," *IEEE Transactions on Wireless Communications*, vol. 2, no. 4, pp. 630-643, 2003, doi: 10.1109/TWC.2003.814353.
- [25] M. Abramowitz and I. A. Stegun, *Handbook of Mathematical Functions with Formulas, Graphs, and Mathematical Tables*, New York, NY, USA: Dover, 1972.

## BIOGRAPHIES OF AUTHORS



**Huu Q. Tran**    received the M.S degree in Electronics Engineering from Ho Chi Minh City University of Technology and Education (HCMUTE), Vietnam in 2010. Currently, he has been working as a lecturer at Faculty of Electronics Technology, Industrial University of Ho Chi Minh City (IUH), Vietnam. He obtained his doctorate from the Faculty of Electrical and Electronics Engineering at HCMUTE, Vietnam. His research interests include wireless communications, non-orthogonal multiple access (NOMA), energy harvesting (EH), wireless cooperative relaying networks, heterogeneous networks (HetNet), cloud radio access networks (C-RAN), unmanned aerial vehicles (UAV), reconfigurable intelligent surfaces (RIS), short-packet communication (SPC), and internet of things (IoT). He can be contacted at email: tranquyhuu@iuh.edu.vn.



**Ho Van Khuong**    received the B.E (with the first-rank honor) and the M.S degrees in Electronics and Telecommunications Engineering from Ho Chi Minh City University of Technology, Vietnam, in 2001 and 2003, respectively, and the Ph.D. degree in Electrical Engineering from University of Ulsan, Korea in 2007. During 2007-2011, he joined McGill University, Canada as a postdoctoral fellow. Currently, he is an Associate professor at Ho Chi Minh City University of Technology, Vietnam. His major research interests are modulation and coding techniques, diversity techniques, digital signal processing, energy harvesting, physical layer security, cognitive radio, and reconfigurable intelligent surfaces. He can be contacted at email: hvkhuong@hcmut.edu.vn.